

Zeitschrift: IABSE publications = Mémoires AIPC = IVBH Abhandlungen
Band: 31 (1971)

Artikel: Lateral buckling of arches
Autor: Asplund, S.O.
DOI: <https://doi.org/10.5169/seals-24215>

Nutzungsbedingungen

Die ETH-Bibliothek ist die Anbieterin der digitalisierten Zeitschriften auf E-Periodica. Sie besitzt keine Urheberrechte an den Zeitschriften und ist nicht verantwortlich für deren Inhalte. Die Rechte liegen in der Regel bei den Herausgebern beziehungsweise den externen Rechteinhabern. Das Veröffentlichen von Bildern in Print- und Online-Publikationen sowie auf Social Media-Kanälen oder Webseiten ist nur mit vorheriger Genehmigung der Rechteinhaber erlaubt. [Mehr erfahren](#)

Conditions d'utilisation

L'ETH Library est le fournisseur des revues numérisées. Elle ne détient aucun droit d'auteur sur les revues et n'est pas responsable de leur contenu. En règle générale, les droits sont détenus par les éditeurs ou les détenteurs de droits externes. La reproduction d'images dans des publications imprimées ou en ligne ainsi que sur des canaux de médias sociaux ou des sites web n'est autorisée qu'avec l'accord préalable des détenteurs des droits. [En savoir plus](#)

Terms of use

The ETH Library is the provider of the digitised journals. It does not own any copyrights to the journals and is not responsible for their content. The rights usually lie with the publishers or the external rights holders. Publishing images in print and online publications, as well as on social media channels or websites, is only permitted with the prior consent of the rights holders. [Find out more](#)

Download PDF: 20.02.2026

ETH-Bibliothek Zürich, E-Periodica, <https://www.e-periodica.ch>

Lateral Buckling of Arches

Flambement latéral des arcs

Seitliches Bogenknicken

S. O. ASPLUND

Göteborg

Synopsis

For analysis the given arch structure is subdivided by joints into a number of finite arch segments. Each arch segment is split in one member above the shear-center and another member below it. The two parts are elastically connected, at the ends of the segment, by torsion stiffener members between the flanges of the upper and lower members, and, along the split web, by a bending resistance member. The elastic properties of each flange in transverse bending, and of the top and bottom members in Saint-Venant torsion, are given by the disconnected member stiffness matrix K . Web member deformations $b - b'$, $b - b'$ and $c - c'$ will be explained later. Horizontal and rotational external spring restraints upon the arch joints are defined.

Those specific joint loads and other conditions for which the buckling safety is sought, are stated. The arch is first analyzed as a stable first or second order theory structure for the loads stated (pre-analysis), resulting in member axial thrusts N and arch moments M .

Thereupon additional degrees of freedom of the joints in lateral buckling are admitted. Structure stiffness matrices are established, U representing the stiffness in elastic bending and twist, and W the thrust effect of N and M and the overturning effects and moment load effects. Eigenvalues equal to the inverse buckling load are finally solved, and their associated displacement modes printed. For practical application the method of the paper is complemented by a computer program. Theory and program are verified by applications to special cases already solved or tested in model by Timoshenko, Stüssi, Weihermüller, and Tokarz or reported by Ojalvo.

Introduction

The subject of lateral buckling of a narrow circular strip was treated by H. HENCKY, Ref. [1], in 1921. S. TIMOSHENKO, in his "Theory of Elastic Stability", Ref. [2], investigates by the energy method the same problem. He adds: "... the energy method ... can be applied ... (to) a curved strip having an *I*-cross section (but it) ... becomes very complicated". Other investigators into the subject have treated various idealized more or less simple cases of arches and loadings. Lately more complete solutions seem to have been undertaken but details have not yet been made available, see FOKOSAWA, DEMUTS, SAKIMOTO, and NAMITA, in OJALVO's List of References, Ref. [6].

F. STÜSSI, Ref. [3], discusses the problem in a quite general way, using his "baustatische" difference equation method.

For any specific arch problem that occurs in practice (variable shape of arch, variable restraints etc.) it is still mostly impossible to find in literature sufficient leads into the design of that arch for adequate buckling safety. The following paper is aimed at establishing a method that should be fairly general and yet manageable in practice, so as to help in filling this need.

Structure and its Members

The initial geometry of the arch is defined by locating its joints 0123 in the *xz*-plane of a coordinate frame *xyz*, see Fig. 1.

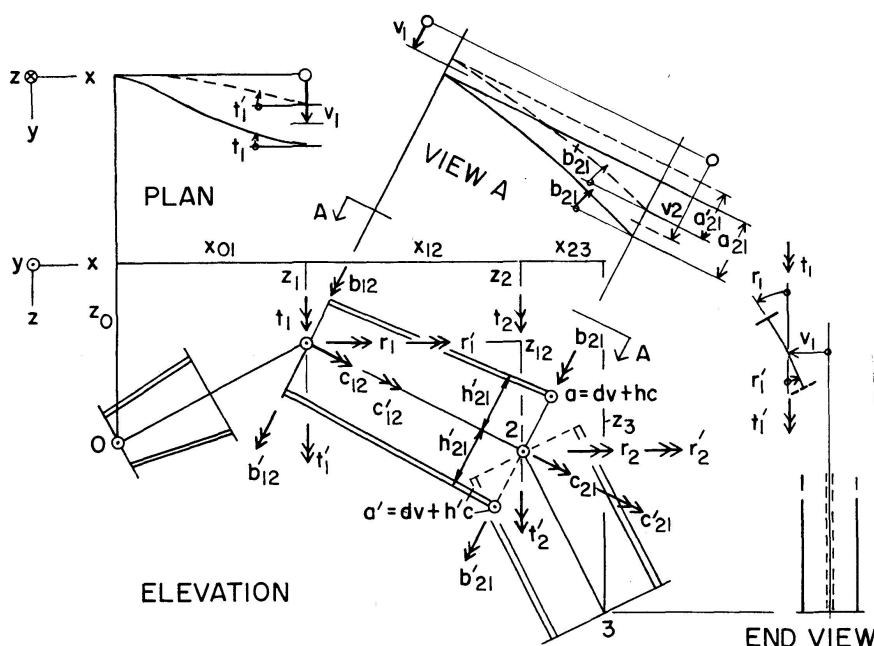


Fig. 1. Views of arch.

Each arch-segment is assumed to have an I cross-section with its web located in a vertical plane. The shear-centers of the segment cross-sections locate the system lines between the geometric joints. The center of the top flange is located at a distance of h above the system line, and the lower flange at h' below. The segment depth is thus $h+h'$.

Stiffness properties of all the members are also given beforehand. Thus also the stiffnesses in transverse ("out-of-plane") bending, $E I$ and $E I'$, are specified for both flanges. Similarly $G J$ and $G J'$ are specified for both beam halves. Stiffness properties for the twist stiffeners and for the bending resistance of the web are also given.

Pre-Analysis

The arch is loaded by those dead and live vertical and horizontal loads P and Q , for which the lateral stability of the arch is sought. The actual plane arch is pre-analyzed for these loads by usual first or second order theory methods. The vertical displacements w of the arch joints, the moments M and the axial forces N in the members, are thus known *before* the following buckling analysis will begin.

The arch is assumed to have a high stability against pure in-plane buckling. Additional vertical joint displacements w occurring *after* the initial state, then can be neglected. Additional horizontal joint displacements u are assumed to have an even smaller influence.

Degrees of Freedom

The state of lateral buckling displacement of the arch structure is indicated in Fig. 1. The geometric segment joints move out-of-plane horizontally in the y -direction by $v = [v_1 v_2]^T$. The upper part of the cross-section rotates by r about a horizontal axis parallel to $0x$, and by t about a vertical axis parallel to $0z$. Both these axes run through the joint. Both rotations $r = [r_1 r_2]^T$ and $t = [t_1 t_2]^T$ apply to displacements of the top flange of the arch. Two *additional* rotations r' and t' in the *same* axes apply to the lower flange. The two flanges of the arch are thus considered in a way as two separate members. The flanges are held together because only one sway is prescribed for the joint, namely v at the geometric web-joint. Two separate angles of rotation c and c' are obtained for the top and bottom flange. The unequal angles of twist of both flanges will give rise to separate Saint-Venant torques in either flanges and a bi-moment torque in the web between the top and bottom flanges.

All degrees of freedom in lateral buckling, or the mode in buckling, are included in the structure displacement vector $p = [v^T r^T t^T r'^T t'^T]^T$.

Member Deformations

For member deformations j are chosen: the sway a_{12} , the left-hand and right-hand end-angles b_{12} and b_{21} , and the angle of twist c_{12} of the top flange members, the corresponding primed variables for the bottom flange, the twist angles $b_{12} - b'_{12}$ and $b_{21} - b'_{21}$ of left-hand and right-hand transverse twist web stiffeners, and the break-in-angle $c - c'$ on the shear-center axis of the web.

Displacement Transformations

The member deformations a depend upon the structure displacements v , r , and t , while a' depend upon v , r' , and t' . The deformations b and c depend upon r and t , while b' and c' depend upon r' and t' , see Fig. 1. Writing as diagonal matrices

$$\begin{aligned} x &= \text{diag}[x_{01} \ x_{12} \ x_{23}], & z &= \text{diag}[z_{01} \ z_{12} \ z_{23}], \\ s &= \text{diag}[s_{01} \ s_{12} \ s_{23}], & s_{12}^2 &= x_{12}^2 + z_{12}^2 \end{aligned}$$

the cosines and sines of the member slopes are found to be

$$\cos \varphi = x_{12} s_{12}^{-1}, \quad \sin \varphi_{12} = z_{12} s_{12}^{-1}, \text{ etc.}$$

Guided by Fig. 1, the displacement transformation E in (1) can now be completed.

$$\begin{bmatrix} a_{01} \\ b_{01} \\ b_{10} \\ c_{01} \\ a'_{01} \\ b'_{01} \\ b'_{10} \\ c'_{01} \\ b_{01} - b'_{01} \\ b_{10} - b'_{10} \\ c_{01} - c'_{01} \end{bmatrix} = \begin{bmatrix} -1 & 1 & -D_{01} & D_{01} & -T_{01} & T_{10} \\ & & -S_{01} & & C_{01} & \\ & & -S_{01} & & C_{10} & \\ & & -C_{01} & C_{01} & -S_{01} & S_{01} \\ -1 & 1 & & & -D'_{01} & -D'_{01} & T'_{01} & -T'_{01} \\ & & & & -S_{01} & & C_{01} & \\ & & & & -S_{01} & & C_{01} & \\ & & & & -C_{01} & C_{01} & -S_{01} & S_{01} \\ -S_{01} & & C_{01} & & S_{01} & & -C_{01} & \\ -S_{10} & & C_{10} & & S_{10} & & -C_{10} & \\ -C_{01} & C_{01} & -S_{01} & S_{01} & C_{01} & -S_{01} & S_{01} & -S_{01} \end{bmatrix} \begin{bmatrix} v_0 \\ v_1 \\ r_0 \\ r_1 \\ t_0 \\ t_1 \\ r'_0 \\ r'_1 \\ t'_0 \\ t'_1 \end{bmatrix} \quad (1)$$

or

$$j_{01} = E_{01} p_{01}$$

with $C_{01} = \cos \varphi_{01}$, $S_{01} = \sin \varphi_{01}$, $D_{01} = h_{01} C_{01}$, $D' = h'_{01} C_{01}$, $T_{01} = h_{01} S_{01}$, $T'_{01} = h'_{01} S_{01}$.

Abbreviating, in the case of three arch elements

$$A = \begin{bmatrix} 0 & 1 & \\ & 1 & \\ & & 1 \end{bmatrix}, \quad B = \begin{bmatrix} -1 & & & \\ & -1 & & \\ & & -1 & 0 \end{bmatrix}, \quad d = A - B = \begin{bmatrix} -1 & 1 & & \\ & -1 & 1 & \\ & & -1 & 1 \end{bmatrix} \quad (2)$$

C , S , h , and $h' = \text{diag}[C_{01} \ C_{12} \ C_{34}]$ etc., would extend (1) into

$$j = \begin{bmatrix} a \\ b \\ b^* \\ c \\ a' \\ b' \\ b^{*'} \\ c' \\ b-b' \\ b^{*}-b^{*'} \\ c-c' \end{bmatrix} = \begin{bmatrix} d & hCd & hSd \\ & -SB & CB \\ & -SA & CA \\ & Cd & Sd \\ d & & -h'Cd & -h'Sd \\ & & -SB & CB \\ & & -SA & CA \\ & & Cd & Sd \\ -SB & CB & SB & -CB \\ -SA & CA & SA & -CA \\ Cd & Sd & -Cd & -Sd \end{bmatrix}$$

where a, b, c, a', b', c' are columns $a = [a_{01} a_{12} a_{23}]^T$ etc., $b^*, b^{*'}$ columns $b^* = [b_{10} b_{21} b_{32}]^T$ etc., and v, r, t, r', t' columns $v = [v_0 v_1 v_2 v_3]^T$ etc.

Member Stiffness Matrix. Member forces

A disconnected stiffness matrix K transforms the member deformations j into member forces J acting upon the member ends: K_B contains the sway stiffness K^t and the transverse bending stiffnesses K of each upper flange member. K^S denotes the Saint-Venant stiffnesses. Primed notations K' , C' , etc. apply to the lower flange members.

$$J = Kj, \quad K = \begin{bmatrix} K^F & & \\ & K^{F'} & \\ & & K^{Web} \end{bmatrix} \quad (3)$$

$$K^F = \begin{bmatrix} K_{01}^t & C_{01}^t & C_{10}^t & C_{21}^t \\ K_{12}^t & K_{23}^t & C_{12}^t & C_{32}^t \\ C_{01}^t & K_{01} & C_{01} & C_{12} \\ C_{12}^t & C_{23}^t & K_{12} & C_{23} \\ C_{10}^t & C_{01} & C_{12} & K_{10} \\ C_{21}^t & C_{32}^t & C_{23} & K_{21} \\ & & & K_{01}^S \\ & & & K_{12}^S \\ & & & K_{23}^S \end{bmatrix} \quad (4)$$

$$C_{01}^t = -(K_{01} + C_{01})s_{01}^{-1}, \quad C_{10}^t = -(C_{01} + K_{10})s_{01}^{-1}$$

$$K_{01}^t = (K_{01} + 2C_{01} + K_{10})s_{01}^{-1}, \quad K_{01}^S = GJ_{01}s_{01}^{-1}$$

$K^{F'}$ similarly as K^F

$$K^{W eb} = \begin{bmatrix} K_{01}^W & & & & & & & \\ & K_{12}^W & & & & & & \\ & & K_{23}^W & & & & & \\ & & & K_{10}^W & & & & \\ & & & & K_{21}^W & & & \\ & & & & & K_{32}^W & & \\ & & & & & & K_{01}^{Wb} & \\ & & & & & & & K_{12}^{Wb} \\ & & & & & & & \\ & & & & & & & K_{23}^{Wb} \end{bmatrix} \quad (5)$$

K_{01}^W holds for web twist, near end, K_{10}^W for web twist, far end, and K_{01}^{Wb} for web bending along arch-segment between flanges.

K and C are the end-stiffness and carry-over stiffness for *the top flange* in weak-axis bending of each member. K^t and C^t are explained in (4).

For uniform (prismatic) members $K_{12} = 4 E I_{12} s_{12}^{-1}$, $C_{12} = K_{12}/2$, and $K_{12}^S = G J_{12} s_{12}^{-1}$, etc. for direct Saint-Venant torsion of the upper part of the cross section. Although it would be mostly poor design, an arch can have an abutment with a *forked support*, permitting a rotation about an axis in the xz -plane that is perpendicular to the first arch member 01. In this case $K_{01} = C_{01} = 0$, $K_{10} = 3 E I_{01} s_{01}^{-1}$, which also affects (4).

Primed stiffnesses K' , C' , K'^t , C'^t , etc. denote magnitudes for the lower flange.

The end-stiffnesses K and carry-over stiffnesses C etc. can be calculated for any stiffness variation and can also be reduced for the effect of axial load that approximately exists at the estimated load when the arch buckles (Berry or van der Fleet functions). This can be omitted for short segments. The effect of shear deformations in the flanges can be included.

Boundary Conditions

Thus, to model a fixed arch with prevented out-of-plane displacements it suffices to nullify $v_0, r_0, t_0, r'_0, t'_0$ and $v_3, r_3, t_3, r'_3, t'_3$ by omitting these components of p together with the corresponding columns of E . Prevented warping is obtained by making K_{01}^W large. To model a forked support and free warping at the springings, hinges are introduced by setting $K_{01} = 0$, $C_{01} = 6 E I/s_{01}^2$, $K_{10} = 3 E I/s_{01}^2$, and the corresponding for the lower flange K'_{01} , C'_{01} , K'_{10} and for the opposite spring element 23. Free warping is obtained by setting $K_{01}^W = K_{34}^W = 0$.

Elastic Structure Loads. Structure Restraints

The member forces J call for structure loads of

$$P = E^T K E p. \quad (5)$$

The arch-joints, Fig. 2, are sometimes braced by side-springs and by rotational springs. Such springs require structure loads of

$$V = S_v v, \quad R = S_r r, \quad T = S_t t, \quad R' = S'_r r', \quad \text{and} \quad T' = S'_t t', \quad \text{or} \quad P = S p \quad (6)$$

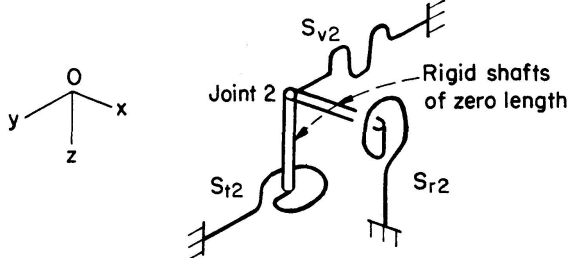


Fig. 2. Spring restraints.

where S are spring constants of obvious magnitudes and dimensions of weight/length and weight by length. For instance, the end-stiffness of transverse bracing of the arch may act as a torsion spring, introducing a moment resistance $R = S_r r$ against twisting of the arch about r . When each joint is connected to a grounded spring, S_v is a diagonal. When on the other hand the arch-joints are connected to another elastic structure, S_v will be the full stiffness matrix of that structure.

We add (5) and (6) into the total elastic structure load

$$P = U p, \quad U = E^T K E + S \quad (7)$$

Thrust Analysis. Displacement Transformation

Just analyzed member forces $J = K j$ are termed elastic. In the next step rigid and straight members between hinged joints are assumed. When the joints displace in buckling, the directions of these rigid bars change. Transverse segment forces are then generated by the member thrusts N and by the flange thrusts $\pm M (h + h')^{-1}$ associated to the pre-analyzed arch moments M .

In the elastic analysis, segment deformations j , namely $a, b, c, a', b',$ and $c', b - b', c - c'$, were used. In the thrust analysis, effort can be saved by excluding the end angles b and b' in bending which are zero and the twists c and c' which have no effect. For the remaining sways a and a' of the flanges, the displacement transformation will be reduced to

$$\begin{bmatrix} a_{01} \\ a_{12} \\ a_{23} \\ a'_{01} \\ a'_{12} \\ a'_{23} \end{bmatrix} = \begin{bmatrix} 1 & D_{01} & T_{01} \\ -1 & 1 & -D_{12} & D_{12} & -T_{12} & T_{12} \\ & -1 & & -D_{23} & & -T_{23} \\ 1 & & & & -D'_{01} & -T'_{01} \\ -1 & 1 & & & D'_{12} & -D'_{12} & T'_{12} & -T'_{12} \\ 1 & & & & D'_{23} & & T'_{23} & \end{bmatrix} \begin{bmatrix} v_1 \\ v_2 \\ r_1 \\ r_2 \\ t_1 \\ t_2 \\ r'_1 \\ r'_2 \\ t'_1 \\ t'_2 \end{bmatrix} \quad (8)$$

or, condensed,

$$i = e p, \quad e = \begin{bmatrix} d & h C d & h S d & 0 & 0 \\ d & 0 & 0 & -h' C d & -h' S d \end{bmatrix} \quad (9)$$

where C, S, h , and $-h'$ are diagonal matrices as in (1).

Axial Force Thrust

The total axial thrust $N + N'$ is first split in two flange thrusts $N = h' n$ and $N' = h n$, where $n = (N + N')/(h + h')$, that is, the total axial force is distributed in inverse proportion to the flange distances.

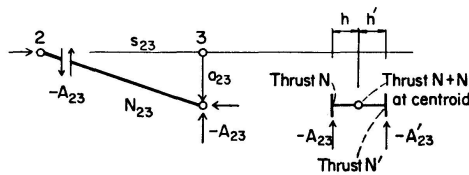


Fig. 3. Thrust stiffness of swayed element.

The flange thrust N_{23} has the inclination $s_{23}^{-1} a_{23}$. For equilibrium, Fig. 3, a transverse force of $-A_{23} = N_{23} s_{23}^{-1} a_{23}$ is required. The thrust-stiffness $F_{23} = -N_{23} s_{23}^{-1}$ is therefore entered into the upper left-hand diagonal of F in (10):

$$I = \begin{bmatrix} A \\ A' \end{bmatrix} = F i = F \begin{bmatrix} a \\ a' \end{bmatrix}, \quad F = - \begin{bmatrix} N + M/(h + h') & 0 \\ 0 & N' - M/(h + h') \end{bmatrix} s^{-1}$$

$$N s^{-1} = \begin{bmatrix} N_{01} s_{01}^{-1} & & & \\ & N_{12} s_{12}^{-1} & & \\ & & N_{23} s_{23}^{-1} & \\ & & & N_{34} s_{34}^{-1} \end{bmatrix}, \text{ etc.} \quad (10)$$

When pre-analyzed horizontal joint-loads Q are zero: $N_{01} s_{01}^{-1} = H_{01} x_{01}^{-1}$, etc.

The complete transformation $V = d^T F a$, $a = d v$ reads for $F = \text{diag} [0 \ 0 \ F_{23} \ 0]$ and $v = [0 \ 0 \ 1]^T$.

$$a = \begin{bmatrix} 1 \\ -1 & 1 \\ -1 & 1 \\ -1 \end{bmatrix} \begin{bmatrix} 0 \\ 0 \\ 1 \\ -1 \end{bmatrix} = \begin{bmatrix} 0 \\ 0 \\ 1 \\ -1 \end{bmatrix}$$

$$\begin{bmatrix} V_1 \\ V_2 \\ V_3 \end{bmatrix} = \begin{bmatrix} 1 & -1 & & \\ & 1 & -1 & \\ & & 1 & -1 \end{bmatrix} \begin{bmatrix} 0 \\ 0 \\ F_{23} \\ 0 \end{bmatrix} = \begin{bmatrix} 0 \\ -F_{23} \\ F_{23} \end{bmatrix} = \begin{bmatrix} 0 \\ N_{23} s_{23}^{-1} \\ -N_{23} s_{23}^{-1} \end{bmatrix}$$

as it should be.

Similarly the thrust stiffness $-N' s^{-1}$ is entered in the lower right-hand diagonal of F .

Moment Thrusts

A bending moment M applied to an I-beam arch-segment of depth $h+h'$ induces a thrust of $M(h+h')^{-1}$ in the top flange and an equally large pull or negative thrust in the bottom flange.

Accordingly, $M(h+h')^{-1}$ is added to N and subtracted from N' in the two diagonal blocks of F in (10).

Thrust Stiffness Matrix

The disconnected thrust stiffness-matrix F is now complete and can be used in forming the structural stiffness matrix of thrust action

$$W = e^T F e + W^{ov} \quad (11)$$

The overturning effect W^{ov} will be next explained.

Overturning Effects

At times some of the vertical loads on an arch are applied upon seats at heights z above the center of the arch joints, Fig. 4. If these part-loads are P , a rotation of the joint by r must be balanced by joint moments of $R = -Pzr$. These add to the thrust stiffness W by a tilting moment $-Pz$ which can be entered in proper sign and position in the matrix W^{ov} in (11). Also horizontal loads can be applied to the joints in such a way that balancing moments of $T = -Qxt$ are needed that are handled similarly.

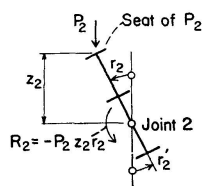


Fig. 4. Overturning load P_2 .

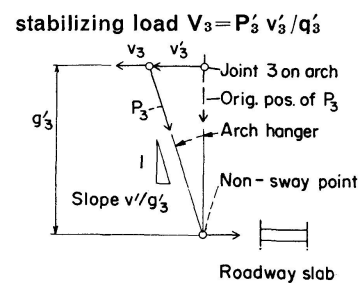


Fig. 5. Changing direction of buckling loads.

At times the directions of the vertical loads (for instance the hanger pulls in an arch) are changed during the buckling progress, Fig. 5. This can be accounted for by adding a stabilizing horizontal load at the joint that is proportional to the hanger load P' and to v' : $V' = (P'/g')v'$. Obviously P'/g' should be added into W^{ov} .

Finally W^{ov} are added to $e^T F e$ in (11).

In other instances an overhead non-sway roadway is supported by columns standing on the arch. In such a case a column load of P and a sway of v will produce an unbalancing force of $V = -(P/g)v$ which is subtracted in (12), for example.

$$\begin{bmatrix} V \\ R \\ T \\ R' \\ T' \end{bmatrix} = \begin{bmatrix} -P/g & & & & \\ & -Pz & -\Delta M & & \\ & -\Delta M & -Qx & & \\ & & & -P'z' & -\Delta M' \\ & & & -\Delta M' & -Q'x' \end{bmatrix} \begin{bmatrix} v \\ r \\ t \\ r' \\ t' \end{bmatrix} \quad \text{or } P = W^{ov} p. \quad (12)$$

Moment Loads

To introduce a stepwise moment diagram into the arch, as was done in (10), external moment loads ΔM must be introduced at the joints equal to the step in moment there. When the structure displaces by r, t , Fig. 6, these external moment loads yield cross-components of $T = -\Delta M r$ and $R = -\Delta M t$ that must be observed. Half or other part $\Delta M'$ of this moment load can be transmitted by the lower arch members governed by the displacements r' and t' , and yielding $T' = -\Delta M' r'$ and $R' = -\Delta M' t'$ which is added in (12).

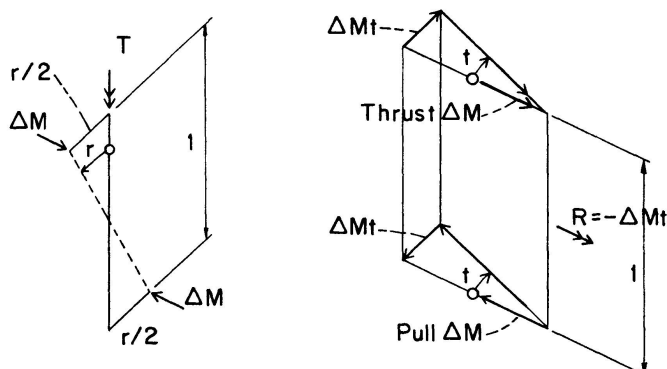


Fig. 6. Response of moment load on arch.

Buckling Condition

The equilibrium conditions for the joints can now be collected into

$$(U + \lambda W)p = P \quad (13)$$

A multiplier λ is introduced for increasing all the pre-analyzed arch loads and results, including thrusts N and $M/(h+h')$ etc., by a common factor. In (13), further, all the structure loads V, R, T, R', T' applied during buckling should

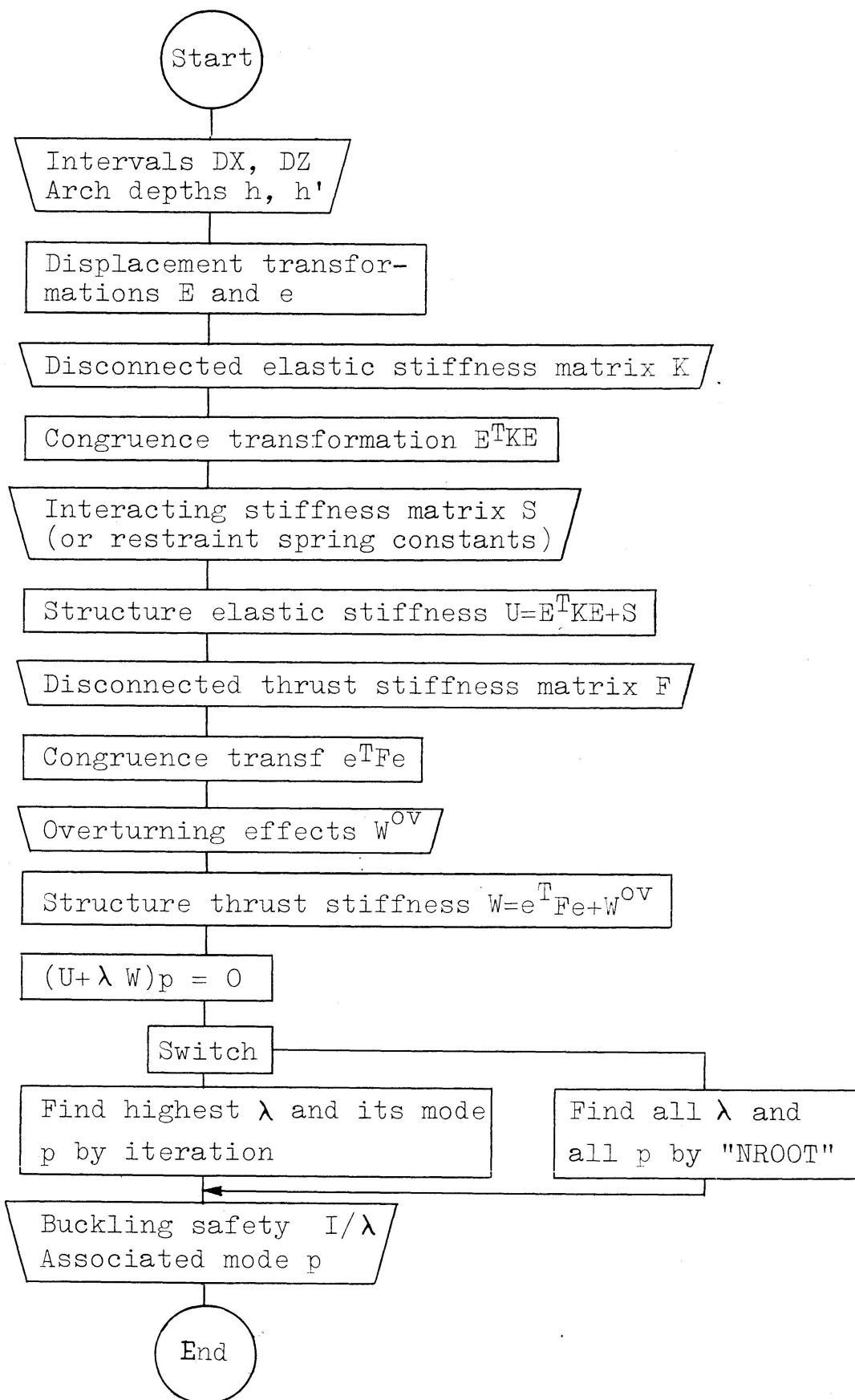


Fig. 7. Flow chart.

be zero. Then (13) has in general only the trivial solution $p=0$. However, for certain discrete values of λ , the eigenvalues, non-trivial solutions p exist.

Eigenvalues and associated modes of buckling are thus solved by the equation

$$(U + \lambda W)p = 0 \quad (14)$$

U and W are symmetric matrices, U representing the elastic stiffness and W the thrust stiffness of the structure. The magnification factor λ increases all applied arch loads until the arch buckles. Therefore λ is also the buckling safety of the given loaded arch.

U has to be invertible and W is generally singular. Eq. (14) can then be transformed into

$$(U^{-1}W + 1/\lambda)p = 0 \quad (15)$$

and solved for the reciprocal eigenvalues $1/\lambda$ and buckling modes p for instance by the Fortran NROOT subroutine or simply by an iterated vector procedure.

Program

Following the course of exposition used in this paper, a straightforward flow-chart is traced in Fig. 7. It was coded in a special matrix language for IBM 1130. For use with for instance IBM/360, their MATLAN matrix language should instead be useful.

Verifications. Conclusions

The theory and programming described is verified in Table 1 by a number of parallel applications to special analyses and model tests reported in litera-

Table 1. *Verifications of Theory*

Test	Sup- ports	Cross- sect.	No. of elem.	Buckl. load calc.	Buckl. load corr.	Ref- ferences
Straight beam in x -direction	Fork	I	4	292	278	Euler 2
Same, in y -direction	Fork	I	4	292	278	Euler 2
Same, in y -direction	Fix	I	4	1350	1110	Euler 4
Straight beam. Constant moment	Fork	I	6	44	43	2, 5
Same. Triang. mom. Bend. stiff web	Fork	I	6	41	39	2, 5
Same. Normal web	Fork	I	6	39	39	
Same. Stiff web. High load	Fork	I	6	27.6	26	2, 5
Same. Low load	Fork	I	6	61	60	2, 5
Parabolic arch $f/l=0,3$, Stüssi, model	Fix	Rect.	6	4.47	4.45	3
Arch $f/l=0,5$, Ojalvo	Fix	Rect.	6	2.92	2.84	6
Arch $f/l=0,5$, Ojalvo	Fix	Rect.	6	2.95	2.84	6
Arch $f/l=0,3$, Weihermüller, model	Fix	I	6	0.300	0.2864	4

ture. Considering the small number of arch-segments (4 and 6) used, the agreement with more or less exact other results seems rather fair. No proper disagreement has appeared. TOKARZ lately has performed a series of tests on the buckling of arches. Fifteen of the buckling loads were verified by the above theory, Ref. [7, discussion], and the agreement seemed fair.

Therefore the conclusion could be ventured that the proposed theory yields fairly correct results in all cases to which it is applicable also when no verification by other methods is obtainable.

A workable elastic theory is often a prerequisite for an inelastic buckling analysis, and it seems possible that the theory and programming given could serve also in a study of inelastic stability.

Symbols

A, a	Member sway couple and sway
B, b	Member end-moments and end-angles
C, c	Member torsion and twist, carry-over stiffnesses, cosine
d	Difference operator
E, e	Displacement transforms, elastic modulus
F, f	Thrust stiffness, rise of arch
G, g	Shear modulus, hanger length
h, h'	Distance of flanges to shear-center
J, j	Member forces and deformations
K, k	Elastic stiffness, Saint-Venant stiffness
l	Length of arch span
$M, \Delta M$	Segment moment, moment load
N, N'	Axial thrust
P, p	Vertical load on joint, or load displacement
Q	Horizontal load on joint
R, r, R', r'	Horizontal moment on joint and rotation
S, s	Spring constants, length of segment, sine
T, t, T', t'	Vertical rotation moment of joint and rotation
U	Structure elastic stiffness
V, v	Out-of-plane load, displacement
W, w	Structure thrust stiffness, vertical arch deflection
W^{ov}	Overturning effects
x, y, z	Orthogonal coordinates or coordinate differences
$1/\lambda$	Buckling safety
	Exponent T denotes transposition

Notation is not fully consistent. Ambiguities are explained also in the text.

References

1. H. HENCKY: Z. Angew. Math. Mech., Vol. 1, p. 451, 1921.
2. S. TIMOSHENKO: Theory of Elastic Stability, 1936.
3. F. STÜSSI: Lateral Buckling and Vibration of Arches, Proceedings IABSE, Vol. 7 (1943), p. 327.
4. H. WEIHERMÜLLER: Zur Berechnung der Kipplast von Bogenträgern (Lateral Buckling Load of Arches), Diss., Darmstadt, Technische Hochschule, 93 p., Darmstadt 1958.
5. S. O. ASPLUND: Lateral Buckling of Beams Without Axial Load, Proceedings IABSE, Vol. 28 (1968), p. 17.
6. M. OJALVO: Out-of-plane Buckling of Curved Members, Draft Oct. 1969.
7. F. J. TOKARZ: Experimental Study of Lateral Buckling of Arches, ASCE Proc. Paper 7893, No. ST 2, February 1971, p. 545 (Discussion p. 2621).

Summary

A general case of laterally buckling arch is analyzed by finite elements. The analysis is programmed for numerical work. Results of programme runs for special types of arches verify buckling loads already solved analytically in literature or obtained by experiments on arches.

Résumé

Un cas général de flambement latéral d'un arc est étudié par la méthode des éléments finis. L'analyse est programmée pour un calcul numérique. Les résultats de programmation pour des types spéciaux d'arcs coincident avec les charges de flambement préalablement obtenues analytiquement dans la littérature ou calculées à partir d'expériences faites sur des arcs.

Zusammenfassung

Es wird ein allgemeiner Fall von seitlichen Bogenknicken mittels endlicher Elemente analysiert. Die Analyse ist für numerische Durchführung programmiert. Die Ergebnisse von Programmierungen für spezielle Bogentypen bestätigen die bereits rechnerisch in der Literatur ermittelten oder die durch Versuche an Bögen erhaltenen Knickkräfte.